Available online at www.sciencedirect.com

ScienceDirect

Energy Procedia 79 (2015) 195 – 203

Energy Procedia

2015 International Conference on Alternative Energy in Developing Countries and Emerging Economies

Computational Modelling of the Flow Field of An Electrolyzer System using CFD

Alhassan Salami Tijani[a]*, Danial Barr[a], A.H. Abdol Rahim[a]

[a]*Faculty of Mechanical Engineering, Universiti Teknologi MARA, 40450 Shah Alam, Selangor, Malaysia*

Abstract

A bipolar plate is one of the primary components in a Polymer Electrolyte Membrane (PEM) electrolyzer which contributes to its hydrogen production efficiency. Its primary function is to distribute the flow of a fluid, in this case water, evenly over the active area of an electrolyzer cell. A well designed and optimized bipolar plate is required to produce an efficient and cost effective PEM electrolyzer stack. In this paper optimal flow plate design and computer models of several available flow plate designs were constructed, and then run through a numerical simulation to evaluate both the hydrodynamic properties they exhibited, the velocity field and pressure gradients. Results indicate that under the specified conditions, the pressure gradient decreases diagonally along the bipolar plate, from the inlet to the outlet. However, the sharpness, or evenness of the pressure gradient varies depending on the design of the bipolar plate. The velocity fields also follow the same general trend, only that they increase in magnitude as they approach the outlet rather than decrease. However, the magnitude of their velocity in the middle of the plates, especially in some of the designs, such as in the multi-pass serpentine designs, varies randomly within a certain range rather than decreasing or increasing evenly, it is only at the outlet that the velocity gradient becomes more consistent. However, of all the designs evaluated the parallel flow field stands out as a very suitable design for use, due to its ability to maintain operational pressures above 1MPa through its entire flow field and also, due to its ability to maintain a stable flow velocity between 3-5m/s, both characteristics which were not displayed by the other two designs. In addition, the parallel flow field design was also able to maintain a average Reynolds number close to the critical value or RE=4000, thus minimizing its internal turbulence.

Peer-review under responsibility of the Organizing Committee of 2015 AEDCEE

*Keywords:*Bipolar plate; Hydrodynamic properties; Simulation; PEM Electrolyzers; Hydrogen production

---

* Corresponding author. Tel.: +601-9624-7571; fax: +603-5543-5177.
E-mail address: alhassan@salam.uitm.edu.my.

Peer-review under responsibility of the Organizing Committee of 2015 AEDCEE
doi:10.1016/j.egypro.2015.11.462

1. Introduction

PEM Electrolyzers are essentially inverted fuel cells, where, instead of generating electricity by harnessing the reaction potential of hydrogen and oxygen to form water, it instead consumes energy to split water into hydrogen and oxygen. The main issue with this device is that it’s components can be costly, thus requiring that designs be tested rigorously by simulation, before they are actually fabricated. It’s cost also hampers the mass manufacture of the device, thus requiring the development of more cost effective designs before this system becomes truly effective.

The hydrodynamic properties of the flow field on the anode side of the electrolyzer stack play an important part in improving the efficiency of the device. A high operating pressure with an even pressure distribution across the reaction surface of the PEM helps to reduce the internal cell resistance, thus reducing the required power output to initiate electrolysis [1]. This also allows for the production of compressed hydrogen gas, thus facilitating storage as noted by Tsiplakides [2]. This is due to the fact that, compressing water consumes much less energy comparing to the energy required for compressing gas state hydrogen as was found by Onda et al [3]. Also of note, is that the gradient of reduction in voltage is the highest between atmospheric pressure and 1 MPa [4] thus, meaning that the pressure threshold for high pressure electrolysis is 1 MPa and above.

Additionally, maintaining a uniform flow field over the reaction surface of a PEM also helps to improve its efficiency and helps to prevent the corrosion of precious catalysts [5]. In order to achieve such ideal conditions, the design of the flow field is once again of paramount importance. The design in question must maintain the aforementioned fluid flow characteristics so as to minimise turbulence within the flow field. In this case turbulence is defined using the Reynold’s number, the resulting number indicates the state of the flow at a particular point in the flow field. For an enclosed channel, similar to a pipe, and the flow channels in a PEM electrolyzer, the values of $Re<4000$ for it to not be turbulent, if the value is $Re<2300$, the flow is completely laminar [6]. However, to note the numbers are soft values, and though they do apply in the case of this study, only an approximation of the flow state is possible. To ensure a uniform flow field with even pressure/velocity distributions as is desired for the optimal performance of the PEM Electrolyzer stack, the proper flow channel design must be utilized. The purpose of the paper is therefore to study the hydrodynamics (pressure and velocity) distribution along the flow field of a PEM electrolyzer. The nature of the flow in the simplified bipolar plate will also be examined so as to ensure minimal turbulence and sufficiently low flow rates of water along the flow channel.

Nomenclature

D	hydraulic diameter of pipe,
A	cross-sectional area
p	wetted perimeter
ρ	the fluid density
R	Reynolds number
V	the mean velocity of the fluid (m/s)
μ	dynamic viscosity of the fluid (kg/s.m)
T	temperature (K) Reynolds number
P	pressure (Pa@N/m^2
u	velocity components in the x coordinate(m/s)
v	velocity components in the y coordinate(m/s)
w	velocity components in the z coordinate(m/s)
x,y,z	coordinate directions with respect to axes(m)

2. Hydrodynamic model of the bipolar plate

A bipolar plate is a structure in a PEM electrolyzer that channels the flow of water over the reactionary surface of the membrane. It is generally constructed out of a metal plate which has grooves machined into it to provide passage for water to flow over the reactionary sites of the membrane. The fluid, in this case, water, is supplied to an inlet and outlet channel machined through the plate, resulting in a flow field as shown in Fig 1. A schematic of the different investigated bipolar plates is shown in Fig 2. Base on the parameters in Table 1, geometrical models were developed in CATIA which were later imported into ANSYS FLUENT software package for simulation and visualization of their flow patterns. When loaded onto ANSYS, the direction of flow for the fields were determined , with the inlet being relatively close to the origin point while the outlet is on a diagonal opposite of the inlet as illustrated in Fig 1. The models we constructed to similar external dimension, with flow field area or approximately $0.01m^2$. Their primary distinguishing features of the flow field channel patterns discussed in this paper are:

- Parallel flow channel
- Serpentine flow channel, single pass
- Serpentine flow channel, double pass

Table 1: Common parameters of the simulated designs

System Parameters	Values/Properties
Flow field surface area	$0.01m^2$
Operating pressure	8 MPa or 80 bar
Operating temperature	27^0C or 300K
Internal wall condition	No slip, Eulerian

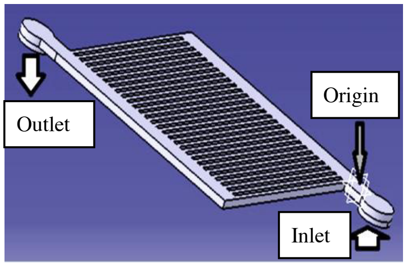

Fig. 1. Flow directions into/out of the flow field

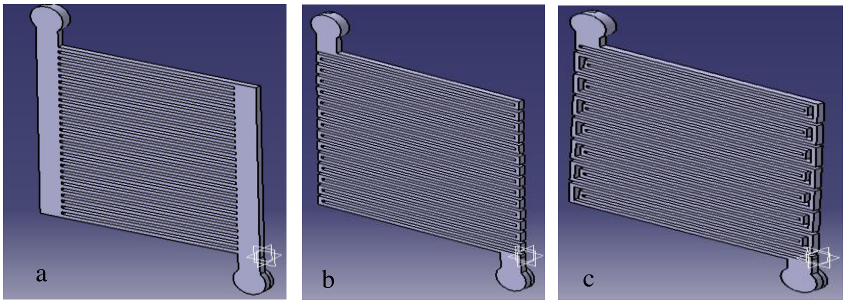

Fig. 2. Bipolar plate models of PEM electrolysis (a) parallel flow field (b) Serpentine flow channel, single pass (c) Serpentine flow channel, double pass

3. Mathematical equations and Numerical methods

In order to determine the flow regimes of the different flow channel designs, we need to utilize the Navier-Stokes equation, which is detailed below.

Continuity equation

$$\frac{\partial}{\partial x}(\rho u) + \frac{\partial}{\partial y}(\rho v) + \frac{\partial}{\partial z}(\rho w) = 0 \qquad (1)$$

Momentum equations

$$\frac{\partial}{\partial x}(\rho uu) + \frac{\partial}{\partial y}(\rho uv) + \frac{\partial}{\partial z}(\rho uw) = \frac{\partial p}{\partial x} + \mu(\frac{\partial^2 u}{\partial x^2} + \frac{\partial^2 u}{\partial y^2} + \frac{\partial^2 u}{\partial z^2}) \qquad (2)$$

$$\frac{\partial}{\partial x}(\rho uv) + \frac{\partial}{\partial y}(\rho vv) + \frac{\partial}{\partial z}(\rho vw) = \frac{\partial p}{\partial y} + \mu(\frac{\partial^2 v}{\partial x^2} + \frac{\partial^2 v}{\partial y^2} + \frac{\partial^2 v}{\partial z^2}) \qquad (3)$$

$$\frac{\partial}{\partial x}(\rho uw) + \frac{\partial}{\partial y}(\rho vw) + \frac{\partial}{\partial z}(\rho ww) = \frac{\partial p}{\partial z} + \mu(\frac{\partial^2 w}{\partial x^2} + \frac{\partial^2 w}{\partial y^2} + \frac{\partial^2 w}{\partial z^2}) \qquad (4)$$

Energy equation

$$\frac{\partial}{\partial x}\left(\rho C_p uT\right) + \frac{\partial}{\partial y}\left(\rho C_p vT\right) + \frac{\partial}{\partial z}\left(\rho C_p wT\right) = k(\frac{\partial^2 T}{\partial x^2} + \frac{\partial^2 T}{\partial y^2} + \frac{\partial^2 T}{\partial z^2}) \qquad (5)$$

The thermosphysical properties are treated as constants and evaluated for water at 27^0C and 8 MPa, density (ρ) = 997.7 kg/m3, dynamic viscosity (μ) = 9.61x10^4 kg/ms specific heat (Cp) =4181.2 J/kg^{0}C thermal conductivity (k) = 0.602 W/m^{0}C).

The Continuity equations detailed above allow us to evaluate several parameters of a flow field, such as velocity and pressure at a particular point in the flow field. This makes the equations indispensable for this paper. However, manual calculation using the formulae can be very tedious, which is why, the process has been conducted using the ANSYS FLUENT software package. This software package was used to obtain the desired results and also to display them in a graphical representation which would simplify the process of interpreting the results.

In addition to the Navier-Stokes equation, the Reynolds number for local region of flow was used to evaluate the turbulence present in the flow. This number is obtained by the use of the following equation.

$$R = \frac{\rho VD}{\mu} \qquad (6)$$

Where:

D= hydraulic diameter of the pipe, or enclosed passage, which, for non-circular cross-sections, is defined as $D = \frac{4A}{P}$, where A is the cross-sectional area, and P is the wetted perimeter, or the total perimeter of the cross-section in contact with the fluid. Again, the ANSYS software package also includes this equation in its visualization packages, thus removing the need for manual calculations.

4. Result and Discussion

The simulation of the design candidates produced results that otherwise fit the initial expectations based on literature reviewed. This helps to provide confidence in the results of the following simulation models. The simulations were modelled to display the following characteristics for analysis;

- Pressure distribution(static pressure)
- Velocity distribution(velocity magnitude)
- Reynold's number contours

The aforementioned values will help in evaluating the flow characteristics of each type of flow field, and how closely they conform to the desired characteristics. The models were tested under a uniform pressure value of 8 MPa or 80 bar to approximate the operating pressures for high pressure electrolysis. As the focus on this study is the effect of flow plate design on flow characteristics, it was determined that the variables should be limited to the design and geometry of the flow field while the initial hydrodynamic characteristics be maintained at a constant value. The following are an elaboration of the results.

4.1. Pressure distribution

The general pattern of pressure distribution across the flow field of all the designs appears to be a gradual drop in pressure diagonally across the flow field from the inlet to the outlet as is visible in the Fig 3(a), (b) and (c).The reason for this drop in pressure can be attributed to several factors, some of them being losses due to drag, or simply due to kinetic losses from in-flow turbulence. However the factors behind the pressure drop are not of as much concern as the effect flow field geometry has on the pressure gradient. Fig 3(d) is an overlay for the pressure gradient of the three designs. The readings were taken along a plane perpendicular to flow direction bisecting the flow field at Z=0.05m. The readings show that the pressure gradient for each design is significantly different, with the parallel flow field displaying the most gradual pressure drop of about 5MPa across the field, while both serpentine variants, that is the single and two-pass fields, record losses of up to 7MPa.

The significance of this is that by conducting electrolysis at pressures beyond a certain threshold, we can reduce the voltage required for the electrolyzer to produce hydrogen gas. As shown in Fig 3(d), this threshold is represented by the red line, which marks a pressure value of 1 MPa. Despite that, electrolysis at higher pressures still result in reduced voltage input, the voltage reduction gradient is not very high beyond the 1MPa threshold. Conversely this means that if the water pressure on the anode of the electrolyzer were to drop below given threshold, it would begin requiring exponentially higher voltages to electrolyze the water into hydrogen gas. Thus it is important that the flow field maintain a gradual pressure gradient to maintain pressures above the threshold for optimised performance.

In this case, it can be observed that parallel flow field is the most successful at the task, consistently maintaining pressure above the threshold across the flow field. In contrast, the other two flow fields consistently lose pressure across the field until it finally dips below the threshold, thus compromising the electrolyzer performance.

4.2. Velocity Distribution

The velocity distribution across a flow field of the anode side of a PEM electrolyzer is not uniform, as is readily demonstrated in the simulations below. In this case however, the behaviour of the flow varies between the flow field types. However, in all the flow fields, the initial and final flow velocity, at the inlet and outlet respectively are the same within each simulation, thus conserving the total flowrate. This lends further validity to the simulation model. However, the individual flowrate within the channels vary between the designs. In Fig 4 (a) for example, the velocity at the channels closer to tha middle are relatively lower, while the channels closer to the sides, and consequently, closer to the inlet and outlet, display higher velocities of flow, and consequently, fster flowrates.
The opposite is true for Fig 4 (b) and (c) which produce a relatively constant fluid velocity along its length, experiencing reductions in velocity only at the bends in the channels. However, something to note is that the magnitude of velocity generated by the Serpentine designs reaches in excess of > 150m/s for the two-pass design and >350m/s for the single pass design. This is visibly illustrated in Fig 4 (d).

As is illustrated in Fig 4 (d) the velocities attained, again, at a plane bisecting the flow region perpendicularly at Z=0.05m, by the serpentine flow field designs are excessively great, to the point at which it might cause damage to the electrocatalyst coating on the MEA. This is beneficial to the operation of an electrolyzer, as the reduced velocity allows the water molecules to interact more readily with the MEA.

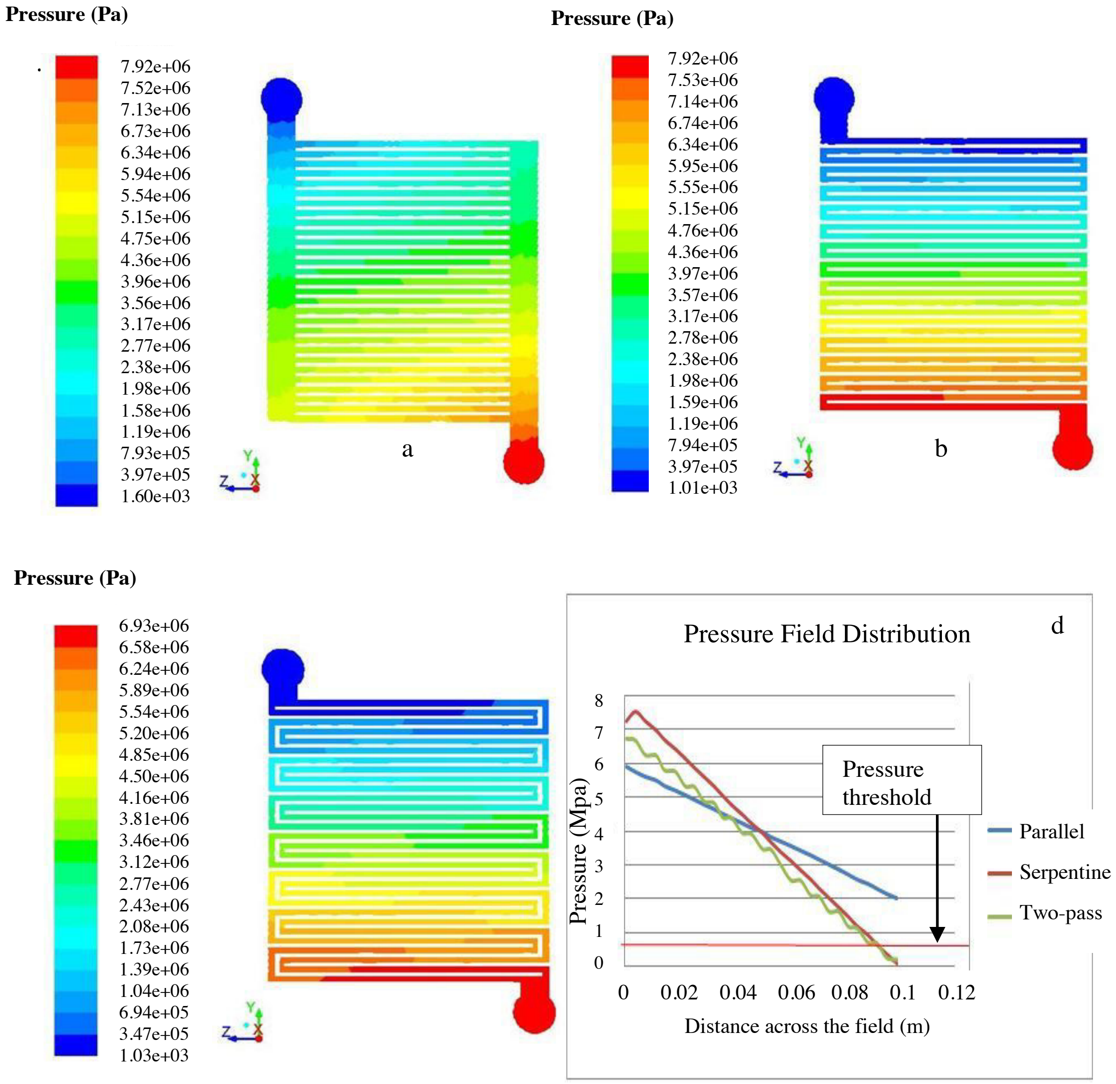

Fig. 3. Pressure distribution across the flow fields (a) parallel flow field (b) serpentine flow field single pass (c) serpentine flow field, (d) pressure gradient of the three designs.

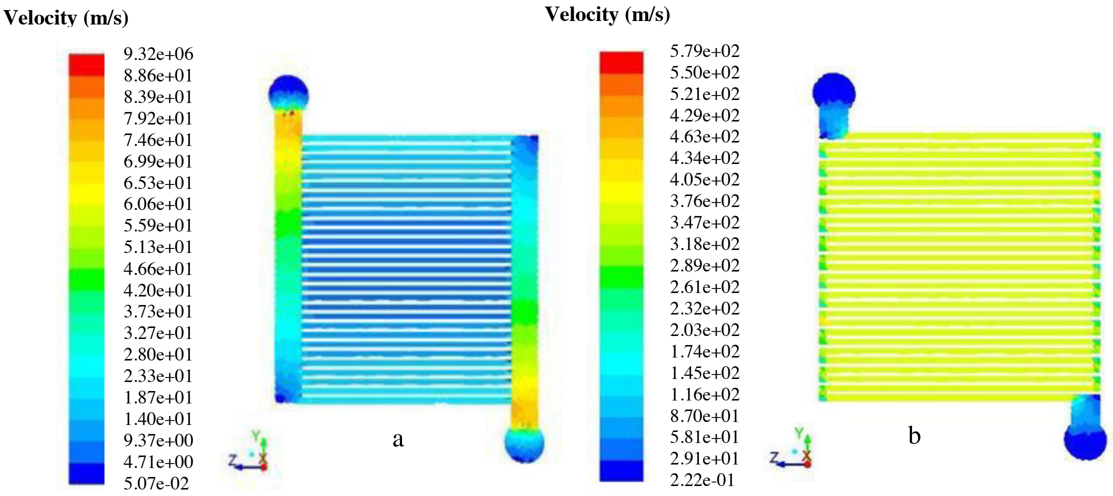

Fig. 4(a),(b). Velocity distribution across the flow fields (a) parallel flow field (b) serpentine flow field single pass

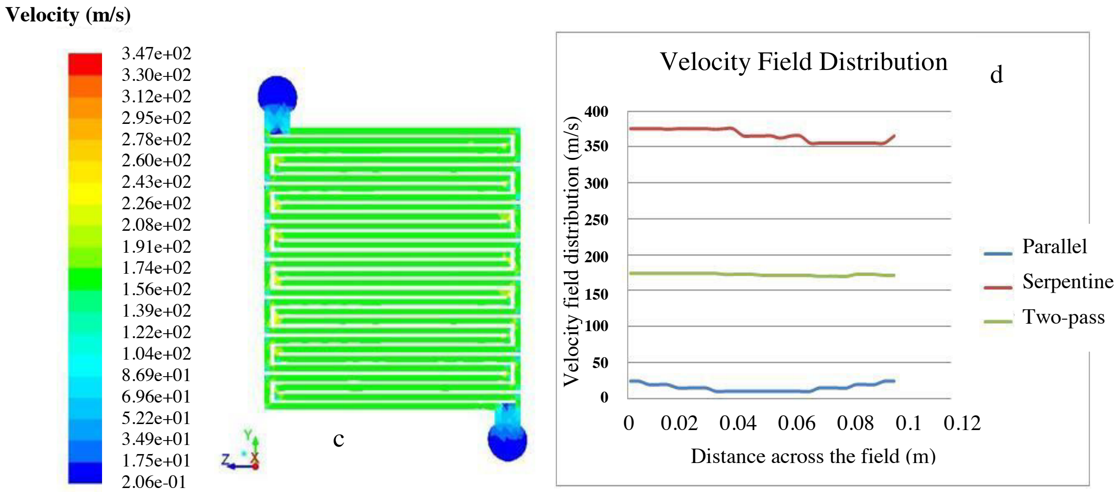

Fig. 4(c),(d). Velocity distribution across the flow fields, (c) serpentine flow field, (d) Velocity distribution across the three designs.

4.3. Contour of Reynolds numbers

Along with the velocity distribution, the Reynold’s number contour was also evaluated. This is primarily in consideration of catalyst erosion due to turbulent flow. The resulting simulations yielded the following results (see Fig 5 (a), (b) and (c)).

As illustrated in Fig 5(a), (b) and (c) the Reynold’s number contours of each design correspond roughly to the velocity contours of the corresponding design, this is unsurprising as velocity, V, is a major variable in calculating the Reynolds number of a given flow region. In an enclosed channel, like those on a flow plate, the critical value of Re before flow becomes turbulent is Re=4000, thus, any value of Re greater than that number indicates turbulent flow in that region. By once again taking values from a plane perpendicularly bisecting the flow region at Z=0.05m, Fig 5(d) illustrate the result. The red horizontal line in Fig 5(d) indicates the turbulent flow threshold in the flow channels. As is apparent, none of the flow channels display non turbulent flow. However, due to the nature of high pressure electrolysis, it is difficult to eliminate turbulence altogether, thus it is only necessary to reduce turbulence to ensure a long operational lifespan for the MEA. In this case the most suitable design to focus on would be the parallel flow field design, since it is the closest to the critical value of Reynolds number, making it possible to minimise electrode erosion if not to eliminate it all together.

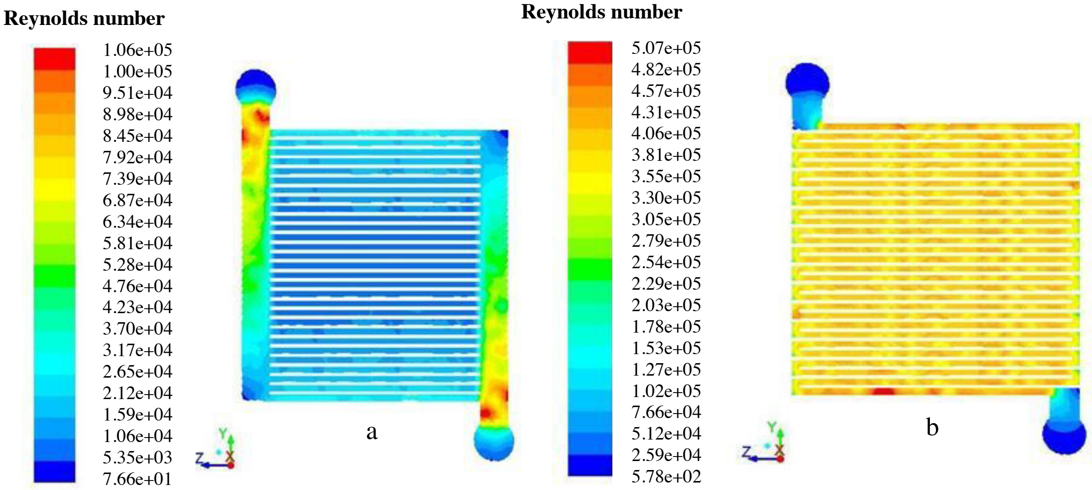

Fig. 5(a),(b). Reynolds number contours (a) parallel flow field (b) serpentine flow field single pass

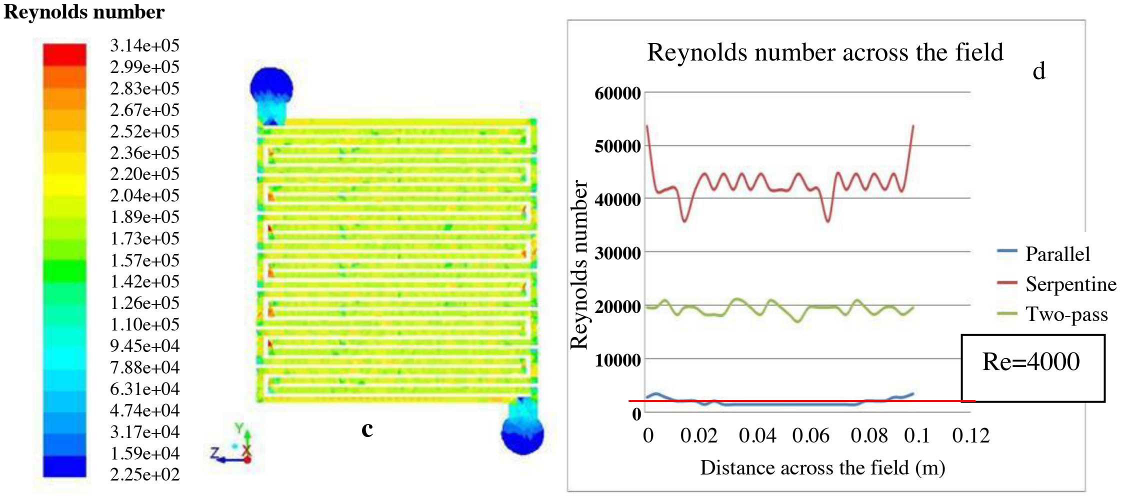

Fig. 5(c),(d). Reynolds number contours (c) serpentine flow field, (d) Reynolds number distribution across flow field of the three designs.

5. Conclusion

The results of this research have contributed greatly to the evaluation of flow channel designs in PEM electrolyzers. In comparing the three models considered, parallel flow channel designs seem to be the most encouraging, with its ability to maintain a stable pressure distribution above the pressure threshold for high pressure electrolysis, as well as its ability to minimise the corrosion of electrocatalysts by ensuring stable, nominal flow rates, and minimal turbulence across the flow field. In addition, the research has also demonstrated the various behaviours of liquid water under high pressure within such systems. This knowledge on these characteristics will contribute greatly in the consideration of future designs for research PEM Electrolyzer flow channels. However, further validation will be required in the future, whether they be in the form of experiments on a prototype to verify other performance criteria, or further simulations to determine the electrochemical aspects of the system, such as the polarizations curves of such a system to determine the viability of pairing the system with renewable energy resources. With the current data at hand, we have a stepping stone on which to continue the development of research electrolyzer systems further.

Reference

[1] Ö. F. Selamet, F. Becerikli, M. D. Mat, and Y. Kaplan, "Development and testing of a highly efficient proton exchange membrane (PEM) electrolyzer stack," *International Journal of Hydrogen Energy,* vol. 36, pp. 11480-11487, 2011.

[2] D. Tsiplakides. PEM water electrolysis fundamentals. Available: http://research.ncl.ac.uk/sushgen/docs/summerschool_2012/PEM_water_electrolysis-Fundamentals_Prof._Tsiplakides.pdf

[3] K. Onda, T. Kyakuno, K. Hattori, and K. Ito, "Prediction of production power for high-pressure hydrogen by high-pressure water electrolysis," *Journal of Power Sources,* vol. 132, pp. 64-70, 2004.

[4] S. K. Mazloomi and N. Sulaiman, "Influencing factors of water electrolysis electrical efficiency," *Renewable and Sustainable Energy Reviews,* vol. 16, pp. 4257-4263, 2012.

[5] J. Nie, Y. Chen, S. Cohen, B. D. Carter, and R. F. Boehm, "Numerical and experimental study of three-dimensional fluid flow in the bipolar plate of a PEM electrolysis cell," *International Journal of Thermal Sciences,* vol. 48, pp. 1914-1922, 2009.

[6] K. T. Trinh. On The Critical Reynolds Number For Transition From Laminar To Turbulent Flow. Available: http://arxiv.org/ftp/arxiv/papers/1007/1007.0810.pdf